The Jahangirnagar Review: Part II: Social Science, Vol. 48, No. 2, 2024
ISSN 1682-7422 © Jahangirnagar University

Pixelizing and Validating Land Surface Temperature from Band 10 of Landsat 8

Md. Ashraful Habib[1]
Faria Kabir[2]
Nur Mohammad[3]

Abstract: The availability of long-term satellite imageries of Landsat since the early 1970s has contributed to a dimensional perspective between the in-situ observatory and ex-situ remote sensors regarding assessing the differences in Land Surface Temperature (LST). This study, therefore, has conducted digital image processing based on Algorithm for Automated Mapping in retrieving the LST and comparing it with the Air Temperature from the weather observatory in Savar, Dhaka, on three distinct occasions. The LST has been obtained from Landsat 8 thermal properties (assigned as band 10 TIRS) and the weather observatory data from Jahangirnagar University campus. The study reveals that there is negligible variation in the timeframe and that it is relatively almost the same fluctuations in the air temperature from the weather observatory. In relation to the Normalized Difference Vegetation Index (NDVI) and Emissivity values, the variability of retrieved LSTs has been evaluated. By processing the time series data, the margin difference evaluated from pixel-based value deviation and point data from the exact location of the weather observatory that was used to determine the relevance of obtaining Land Surface Temperature which can be changed by taking into account the atmospheric influence and weather conditions of seasonal fluctuations. The goal of the current study has been derived from the Raster Calculation method to retrieve data to validate with air temperature. The method is effective by providing a difference of ±0.5˚C on the study, according to the difference between the LST and air temperature, which indicates a prominent phase of retrieving temperature data for the vast accumulation of climate-based research.

Keywords: LST; Weather Observatory; Landsat 8; Pixel-based Analysis; NDVI.

1. Introduction

In remote sensing, Landsat thermal bands are used to extract temperature from a certain wavelength with a Digital Number (DN), which is then translated into spectral radiance, which is the fundamental unit of temperature. This study explore a unique application of remote sensing in Bangladesh by contrasting the land surface temperature and air temperature from weather observatories. The thermal band in Landsat for surface temperature inquiry and application still untapped which is notably mentionable when addressing land surface temperature (LST). Most Landsat TM thermal data evaluations to date have focused on the reliability of concerning the brightness temperature or DN value

---

[1] Lecturer, Department of Geography and Environment, Jahangirnagar University, Savar, Dhaka-1342
[2] Research Associate, Centre for Climate Change and Environmental Research (C3ER), BRAC University.
[3] MSc Research Student, Institute of Cartography and Geoinformatics, Eötvös Loránd University (ELTE), Hungary.

to problems in the reality as well as on sea surface temperature study adjusted using the atmospheric model (Qin, Karnieli, & Berliner, 2001).

Regardless of the study's scope, remote sensing extends the chance to provide a consistent and repeatable procedures that is appropriate for both short-term pilot studies and long-term monitoring projects. Despite their high initial cost, remote sensing platforms are much superior to traditional fieldwork campaign studies due to the simplicity of data access to end researchers and the frequently large temporal and spatial coverage provided (Tomlinson et al., 2011). In order to use data accurately and effectively for weather sensing, it is important to understand the theory underlying the derivation of LST from distant sensing methods, which is covered in this section. The physics behind determining LST is given in greater detail if more information is needed (Dash, Göttsche, Olesen, & Fischer, 2002). Alternatively, the specifications of specific platforms or sensors can be examined (Tomlinson et al., 2011). Bangladesh currently faces inescapable problems related to global warming and long-term climatic and environmental changes as a result of rising temperatures. In Bangladesh, air temperature data obtained from weather stations are typically used to evaluate weather forecasts and meteorological data, but this data is not always accurate or authentic due to poor administration.

All places and areas do not have stations because specific spatial and meteorological tools are very expensive and are not adequately maintained. As a result, researchers now use remote sensing software to obtain more reliable data. Understanding the terms Land Surface Temperature and Surface Air Temperature is necessary to defining the actual condition of temperature, rise, and advancement. The application of satellite-based land surface temperature estimation can aid in outlining the geographical problem of estimating surface air temperature, remarkably in regions with low station density. The full probability of the current climatological change can be explained by contrasting the two forms of data.

The inter-comparison approach solely evaluates the satellite-derived LST in comparison to another well-validated LST product. Without requiring any ground measurements, this approach can be applied everywhere if such a well LST product is accessible. Land surface temperature (LST) is significant in agricultural research, urban heat island effects, and monitoring of environmental issues. But, with the introduction of a succession of remote sensing satellites, significant progress has been achieved in these applications. Several geophysical variables were assessed using LST divergences in space and time detected by satellite remote sensing data. To justify the established method, efficiency must be verified in relation to the real database. This approach will ensure data gathering in areas where weather stations have not been constructed. In Bangladesh, the use and analysis for obtaining temperature using remote sensing will have a significant effect on future studies. The validations support the correctness and represent proper procedures, implying that this study will have a significant role in this region. This study aims to obtain the Land Surface Temperature from Thermal Band on Landsat and evaluate it with Air Temperature collected from weather observatory stations to analyze the variation by the algorithm. The respective objectives are to generate temperature from spectral signatures of certain study areas in Bangladesh from Landsat Thermal Band; to integrate remote sensing and weather station data in pixels and ground observatories respectively nearby comparable areas; and to assess and validate thermal band and field observatory data using USGS Land Surface Temperature formulating algorithm and then extend the techniques at different regions across the country level.

2. Methodology

2.1 Study Area

This research is relevant to the changes in LST in Savar Upazila, which experiences similar weather conditions as the Dhaka city and metropolitan area. Savar Upazila (having 286 km^2 area) is situated between 23°44' and 24°02' N latitudes and 90°11' and 90°22' E longitudes. The land is composed of Pleistocene alluvium, and the elevation gradually increases from east to west. The southern part of the Upazila is formed from alluvial soil from the Bangshi and Dhaleshwari rivers. The primary rivers in the Savar area include the Bangshi, Turag, Buriganga, and Karnatali (Saha, 2012). Industrial garbage has polluted the Bangshi. Savar Upazila had a population of 1385910. (BBS, 2011).

Dhaka experiences a tropical climate characterized by hot, wet, and humid weather, falling under the tropical wet and dry climate category according to the Köppen climate classification. However, wetlands and bodies of water in and around Dhaka are being converted to buildings and other establishments, leading to environmental degradation and loss of biodiversity. The city's population, currently at 13 million, is expected to rise to 20 million by 2025. Due to excessive carbon emissions and pollution, Dhaka is considered the most vulnerable city in Bangladesh. Air and water pollution have reached alarming levels, with the population increasing over decades and density almost quadrupling. This population growth has led to changes in various land cover classifications, with habitat structures following major roadways as well as industrial hubs.

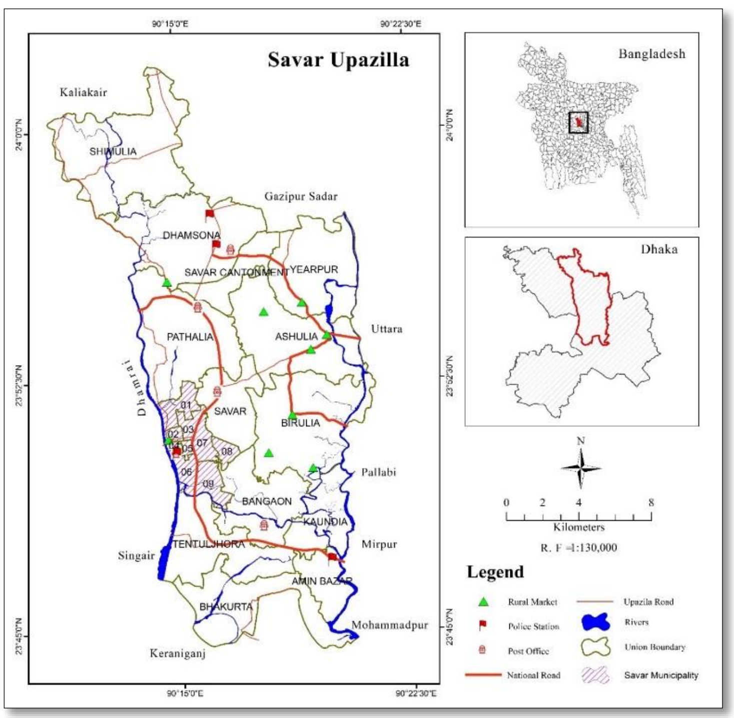

Figure 1: Location of Savar upazila, Dhaka district with rivers, prominent places, and municipality zone. Source: Compiled by author from BBS data, 2023

2.2 Dataset for LST and Remote Sensing Techniques

The study had required the Cloud-free satellite imagery data of Savar, that's why Landsat 8 on particular years of 2014, 2018 and 2023 had been collected. The imageries had been offered on the US Geological Survey website. Since the imageries had been chosen cloud free during image acquisition, though the atmospheric correction was not performed. The Landsat data were pre-georeferenced products that were corrected for geographical research. The spectral characteristics with band wavelengths and resolution of the satellite imageries are 30 m, while Google Earth pictures had a resolution of 5 m (Avdan & Jovanovska, 2016).

Table 1: Data Type and Source

Data Type	Data Name	Scale	Date/ Duration	Source
Satellite Imageries	Landsat 8 OLI	February,	2014, 2018, 2023	USGS/ Earth Explorer https:// search. earth data. nasa. gov/
GIS Layers	District and Upazila Borders, Urban Land use	1: 130,000	2016	LGED Upazila Base map and CEGIS

Source: CEGIS, 2021; usgs.gov, 2023

Table 2: Characteristics of Satellite Imageries with Band Combinations

Data Type	Date	Path/Row	Reflectance Channels Spatial Resolution	Thermal Channels Spatial Resolution	Thermal Band (Band number with Wavelength)
Landsat 8 OLI	10 February 2014 21 February 2018 11 February 2023	137/44	30 meters	100 meters	Band 10 (10.60 - 11.19µm)

Source: usgs.gov, 2023

2.3 Formulas for Retrieving LST from Landsat 8

According to Irons et al., 2012 and Forbearance, 2013, thermal TIRS bands, are used to facilitate atmospheric modification of thermal data when utilizing the Split Window Algorithm. McMillin was the first to suggest the Split Window Algorithm, and he presented variations in atmospheric absorbance of two bands for retrieving Sea Surface Temperature to the letter. The primary principle behind this approach, according to José A. Sobrino et al. (2008), is the attenuation from radiance for air absorption, which is inversely proportional to the advance change at two separate wavelengths.

LST is obtained by adjusting the brightness temperature to account for spectral emissivity. The Artis and Carnahan (1982) algorithm was used to estimate the emissivity-adjusted LST; emissivity adjustment is determined by the type of land and is performed by using NDVI values for each pixel.

Table 3: Specifications of Image Bands in Landsat 8

Satellite	Band	Wavelength (µm)	Resolution (m)
Landsat- 8 OLI (Operational Land Imager) and TIRS (Thermal Infrared Sensor)	Band 1- Ultra Blue	0.435- 0.451	30
	Band 2- Blue	0.452–0.512	30
	Band 3- Green	0.533–0.590	30
	Band 4- Red	0.636–0.673	30
	Band 5- Near Infrared (NIR)	0.851–0.879	30
	Band 6- Shortwave Infrared (SWIR) 1	1.566–1.651	30
	Band 7- Shortwave Infrared (SWIR) 2	2.107–2.294	30
	Band 8- Panchromatic	0.503–0.676	15
	Band 9- Cirrus	1.363–1.384	30
	Band 10- Thermal Infrared (TIRS) 1	10.60–11.19	100 * (30)
	Band 11- Thermal Infrared (TIRS) 2	11.50–12.51	100 * (30)

Source: usgs.gov, 2023

The mathematical description of the regulative Algorithm is emphasized. The Landsat 8 data can be found on the Earth Explorer website. Techniques for calculating the necessary essential parameters are also detailed in the study, making it straightforward to apply the algorithm in practice. The ground emissivity is calculated using Landsat 8 land cover data, while the other two parameters are computed using climatological factors (Avdan and Jovanovska, 2016). When the NDVI is less than zero, water is determined to be the type of land cover, and an emissivity estimate of 0.991 is assigned. The land cover type is assumed to be soil when the NDVI is between 0 and 0.2, and an emissivity value of 0.966 is noted. A unique equation is used to calculate the emissivity when the NDVI is between 0.2 and 0.5, which is reflected by a combination of soil and vegetation cover. Vegetation cover is examined when the NDVI exceeds 0.5, and a value of 0.973 is reported (Kamran et al., 2015).

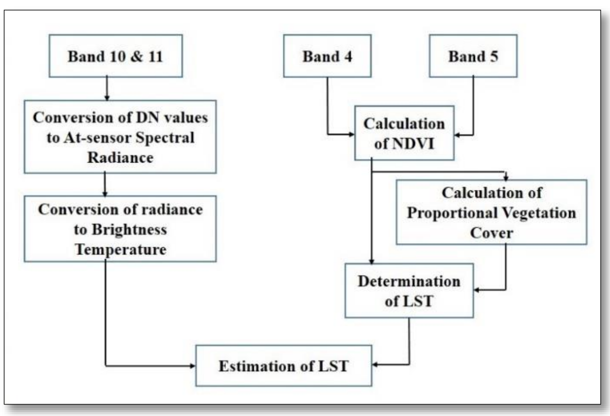

Figure 2: Flowchart of Methods to conduct LST from Landsat 8. Source: Kamran et al., 2015.

In this study, the NDVI was measured using bands 4 and 5, and the brightness temperature was estimated using TIR band 10. Table 4 contains the metadata for the satellite imageries applied in the algorithm. The metadata is included in the bundle of satellite images, and exact notations for each value and wavelength are explicitly stated.

Table 4: Metadata of Landsat 8

Thermal Constant, Band 10	K_1	1321.0789
	K_2	774.8853
Rescaling Factor, Band 10	M_L	0.000342
	A_L	0.1

Source: usgs.gov, 2023

Use the USGS approach to compute the LST the computations were carried out using the software ArcGIS, specifically the ArcMap 10.6.1 version (Avdan & Jovanovska, 2016).

(1) Calculation of Top of Atmospheric (ToA)

Band 10's contribution is the algorithm's initial stage. After inserting band 10 into the backdrop, the application uses the following USGS website computations to assess the top of atmospheric (TOA) spectral radiance (L):

$L\lambda = M\ L * Q\mathbf{cal} + A\ L - O\ i$ ....**(**Kamran et al., 2015)

where M L denotes the band-specific multiplicative rescaling factor, Qcal the Band 10 picture, A L the band-specific additive rescaling factor, and O i the Band 10 correction.

Computation View of Algorithm:

TOA = 0.0003342 * “Band 10” + 0.1 ....**(**Kamran et al., 2015)

(2) Calculation of Conversion of Radiance to At sensor Temperature (BT)

The TIRS band data should be transformed from spectral radiance to brightness temperature (BT) utilizing the thermal constants from the metadata file after converting the digital numbers (DNs) to reflectance. The algorithm of the tool converts reflectance to BT using the following equation:

$\mathbf{BT} = K_2 \ln [(K_1 / L\lambda) + 1] - 273.15$ ....**(**Kamran et al., 2015)

where K 1 and K 2 are the identified band-specific thermal conversion constants.

The radiant temperature is adjusted by combining it with absolute zero (about 273.15°C), giving the results in Celsius.

Computation View of Algorithm:

BT = (1321.0789 / Ln ((774.8853 / “TOA”) + 1)) – 273.15.......................**(**Kamran et al., 2015)

(3) Calculation of Emissivity Correction with NDVI

Calculating NDVI: The visible and near-infrared bands of Landsat were utilized to generate the Normal Difference Vegetation Index (NDVI). The NDVI must be estimated since it can be employed to infer overall vegetation environment and the amount of vegetation is a critical driver. The NDVI calculation must be correct in order to compute the vegetation proportion (PV), which is related to the NDVI, and emissivity, which is related to the PV:

NDVI = NIR (band 5) – R (band 4) / NIR (band 5) + R (band 4) ....**(**Kamran et al., 2015)

Where NIR stands for near-infrared (Band 5) and R stands for red (Band 4).

Computation View of Algorithm:

NDVI = Float (Band 5 – Band 4) / Float (Band 5 + Band 4)................**(**Kamran et al., 2015)

Calculating the Proportion of Vegetation (PV): In order to apply to planetary conditions, the suggested approach for calculation recommends using the NDVI values for vegetation and soil (NDVIV = 0.5 and NDVIs = 0.2):

$\mathbf{PV = (NDVI - NDVI}s\ \mathbf{NDVIV - NDVI}s\mathbf{)}$ ....**(**Kamran et al., 2015)

Despite the fact that NDVI values differ from place to place, the assessment for vegetated surfaces, 0.5, may also be insufficient. Since NDVIV and NDVIs are dependent on atmospheric conditions, an NDVI computed utilizing TOA reflectivity would not be able to produce global values. Instead, at-surface reflectivity can be applied to calculate global NDVI values.

Computation View of Algorithm:

$\mathbf{P_v = Square\ ((NDVI - NDVI_{min}) / (NDVI_{max} - NDVI_{min}))}$........**(**Kamran et al., 2015)

Calculating Land Surface Emissivity: Knowing the land surface emissivity (LSE), which scales blackbody radiance (Planck's law) to estimate emitted radiance, is necessary to predict LST because it measures how well thermal energy is transmitted. The following calculations are made to determine the ground emissivity conditionally:

$\varepsilon\lambda = \varepsilon V\lambda\, PV + \varepsilon s\lambda\, (1 - PV) + C\lambda$ ....**(**Kamran et al., 2015)

Where εV and εs represent plant and soil emissivity, respectively, and C represents surface roughness (C = 0 for homogeneous and flat surfaces) as a constant value of 0.004.

Water is classified when the NDVI is less than 0 and an emissivity value of 0.991 is provided. An emissivity rating of 0.996 has been assigned when the NDVI is between 0 and 0.2, which indicates that soil covers the terrain. Values between 0.2 and 0.5 are categorized as soil and vegetation cover combinations when determining the emissivity. When the NDVI value is greater than 0.5, vegetation is deemed to be present, and a value of 0.973 is assigned.

Computation View of Algorithm: $\varepsilon = 0.004 * P_v + 0.986$......................**(**Kamran et al., 2015)

(4) This is the method for calculating the emissivity-corrected land surface temperature T s, also known as the crucial phase in LST extraction:

$Ts = BT\ \{1 + [(\lambda BT/\rho)\ \ln \varepsilon\lambda]\}$.....................................**(**Kamran et al., 2015)

Where Ts is the LST in degrees Celsius (C), BT is the at-sensor BT (C), is the emission wavelength (for which the highest emission and the average of the constraining wavelength (=10.895) will be utilized), and is the projected emissivity, and

$\boldsymbol{\rho = h\ c\ \sigma = 1.438 \times 10\ {-2}mK}$ ....(Kamran et al., 2015)

Where h is the Planck's constant (6.626 1034 J s), c is the speed of light (2.998 108 m/s), and σ is the Boltzmann constant (1.38 1023 J/K).

Computation View of Algorithm:

LST = (BT / (1 + (0.00115 * BT / 1.4388) * Ln(ε)))....................(Kamran et al., 2015)

Although this method has frequently been employed in LST recovery using a number of sensors, it does not require exact knowledge of the atmospheric profiles during satellite capture. After estimating the LST, the research areas were trimmed from Arc Toolbox's Raster Processing in ArcMap 10.6. Following that, each satellite image is exported to a map (Avdan & Jovanovska, 2016). Following that, the three-day maps of each research region were marked with the position of the weather station. Also, the relevant point value has been highlighted with a marker in order to obtain more Land Surface Temperature measurements.

2.4 LST Validation

The demonstrated tool used more data and took both the average temperature and the definite temperature in the specified pixel at the time of the satellite crossing over the area for the 137/44 path-row along with representative points for the authentication of the final retrieved LST results. Even though the resolution of LANDSAT 8 for the bands utilized is 100m for the thermal band and 30m for the red and NIR bands, the comparison was conducted using air temperature, which is distinct and can occasionally make huge variations. The LST was approximated and recorded at pixel where the monitoring location was situated.

3. Results

3.1 Changes in Land Surface Temperature in Different Years

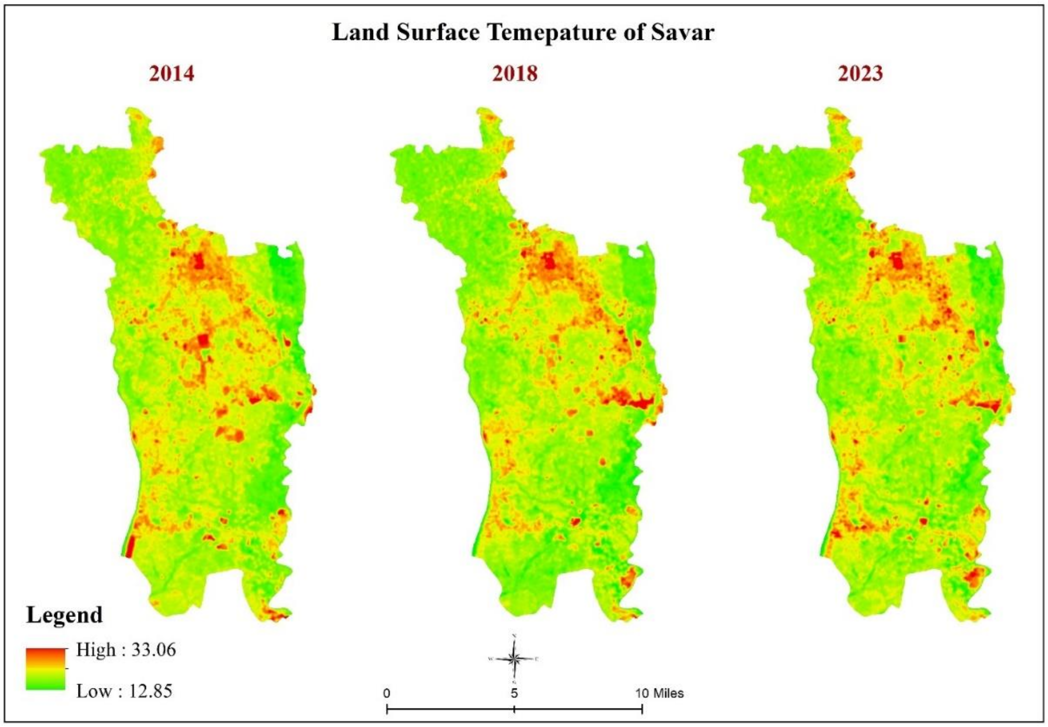

Figure 3: LST in 2014, 2018, and 2023. Source: Compiled by author from usgs.gov, 2023.

Figure 3 illustrates the visualized concept of LST changing in different years, as well as how the LST changed, as shown in Table 5. 30 locations had been selected for determining the observation about the changes that happened. Static changes are observed as LST values are higher in 2018 than 2014 values, on other hand, 2023 values are lower than 2018 in a smaller scale. About ±3˚C changes occurred between 2014 and 2018. Apparently, temperatures are lower in 2023 than 2018 with ≥1˚C. Some points have a regular increase in LST in 2018.

Table 5: LST Changes in Different Years

Point	Latitude	Longitude	LST		
			10-Feb-14	21-Feb-18	11-Feb-23
1	23°59'40.48"N	90°12'21.43"E	21.27	23.5	22.74
2	23°56'46.95"N	90°15'49.35"E	23.57	25.69	24.19
3	23°54'4.69"N	90°19'4.68"E	22.71	24.02	22.8
4	23°50'20.06"N	90°15'29.48"E	23.52	25.81	24.83
5	23°50'23.75"N	90°19'37.35"E	21.4	24.44	23.85
6	23°47'38.42"N	90°18'52.42"E	22.37	25.1	24.28
7	23°47'50.85"N	90°15'41.57"E	22.77	25.39	24.85
8	23°51'45.10"N	90°16'43.69"E	22.6	25.42	23.04
9	23°55'55.40"N	90°18'24.26"E	24.38	26.63	25.74
10	23°50'3.55"N	90°17'48.10"E	22.29	23.77	22.74
11	24° 0'13.02"N	90°14'26.62"E	21.67	23.88	22.8
12	23°58'34.76"N	90°12'38.32"E	21.91	24.1	23.25
13	23°55'49.44"N	90°16'31.92"E	22.92	25.63	24.22
14	23°54'6.21"N	90°17'4.65"E	27.47	27.08	28.1
15	23°55'9.40"N	90°14'8.80"E	22.5	24.82	24.12
16	23°52'7.42"N	90°20'26.56"E	20.73	28.33	26.08
17	23°51'36.29"N	90°17'48.35"E	26.04	27.65	26.1
18	23°57'29.91"N	90°17'15.00"E	22.77	24.5	23.08
19	23°49'29.50"N	90°16'33.61"E	24.31	25.3	24.88
20	23°49'3.86"N	90°19'30.97"E	19.43	22.23	20.96
21	23°45'49.95"N	90°19'35.91"E	22.06	24.56	24.01
22	23°48'47.70"N	90°18'16.64"E	21.73	24.1	23.06
23	23°45'26.55"N	90°16'20.57"E	22.9	24.56	24.21
24	23°48'46.58"N	90°17'1.10"E	21.72	25.35	24.45
25	23°53'23.72"N	90°14'8.54"E	22.57	24.34	23
26	23°53'23.46"N	90°16'57.65"E	25	26.91	24.89
27	23°52'36.65"N	90°17'58.16"E	22.6	24.64	22.6
28	23°58'29.45"N	90°14'29.94"E	21.41	23.41	22.06
29	23°46'58.30"N	90°17'29.66"E	21.38	23.59	22.8
30	23°46'30.87"N	90°15'39.60"E	22.68	24.57	23.6

Source: Compiled by author from usgs.gov, 2023

3.2 LST Validation with Weather Observatory Data

The comparison was made using the air temperature at weather station, which is not the same and occasionally subject to significant variations due to LANDSAT 8's thermal band resolution of 100 m and optical band resolution of 30 m. The LST for the pixel containing the weather station was calculated and noted. The differences can also be related to the features of the sensor and the weather (Kamran et al., 2015). For the considered study area, only one meteorological station had been measured for the validation process. As the weather observatories in Bangladesh are not sufficient for collecting Surface air temperature, huge areas are included in the average temperature value, whereas different land covers directly impact heat generating and reflected radiations. The difference between the recorded LSTs and the air temperatures and specifics on the station had been tabulated in Table 6 with the proper database presentation of Dry bulb, wet bulb, maximum temperature, minimum temperature, and mean temperature of 3 hours values on each day. Furthermore, the study area is in Dhaka, the capital city. That's why the LST differences are quite prominent due to many circumstances.

Table 6: Detailed Differences between LST and Weather Observatory Temperature

Weather Observatory Name	Latitude	Longitude	Date	Weather Observatory Data (°C)					LST (°C)	Difference (WO Mean Temp.- LST) (°C)	Remarks
				Dry Bulb	Wet Bulb	Max. Temp.	Min. Temp.	Mean Temp.			
Jahangirnagar University, Savar, Dhaka 1342	23°52' 40.41" N	90°16' 10.63" E	10 February 2014	23.6	20	26.6	20	23.3	22.63	0.67	Slightly Extension
			21 February 2018	27.3	24.3	29	20.3	24.65	24.65	0	Accurate Value
			11 February 2023	23.7	22.7	30.3	15	22.65	22.77	-0.12	Value slightly decayed

Source: Compiled by author from usgs.gov, 2023

From the analysis, of the three different dates in the same month in different years, the anticipated difference has been clarified. The LST of the weather observatory point from 2018 had been validated with the same mean temperature. On the other hand, LST was only 0.67 lighter than the surface temperature, but on the opposite, the recent data of 2023 has been slightly mightier with a 0.12 value. Moreover, the substantial values with dry bulb and wet bulb indicate the various level of surface temperature at different times and heights. Maximum and minimum temperatures are included in the factors of reflection level on the particular ground stations. The analysis had been done in a complex method and the particular one-pixel value indicates one weather observatory. The detailed methods had been thoroughly followed, where NDVI corrections for proportionate vegetation, as well as emissivity, had been calculated with definite coefficient values largely utilized in metaphysics and terminal functions (Kamran et al., 2015). The following Figures 4, 5, and 6 are the clarifications for the exact valid point for the accuracy assessment of the conducted LSTs of different dimensions. For instance, satellite imageries provide vast information with band wavelength and definite formulas, but some factors like cloud cover create obstacles to getting a clear version with high-resolution images.

This study offers guidelines on best practices for LST product validation. To maintain interoperability between products and reference data sets, internationally recognized definitions of LST, emissivity, and associated numbers are given. According to an assessment of present validation capabilities, progress is being made in terms of upscaling and in situ measuring methodologies, but there is inadequate uniformity in terms of performing and reporting statistically robust comparisons. Emissivity and surface temperature aid in a better comprehension of the general land classes in metropolitan areas, which in turn aids in a better comprehension of energy budget difficulties.

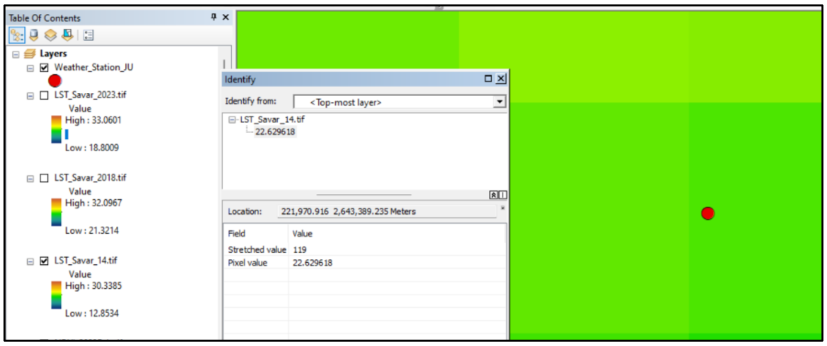

Figure 4: Validation of LST for 2014, Source: Compiled by author from usgs.gov, 2023

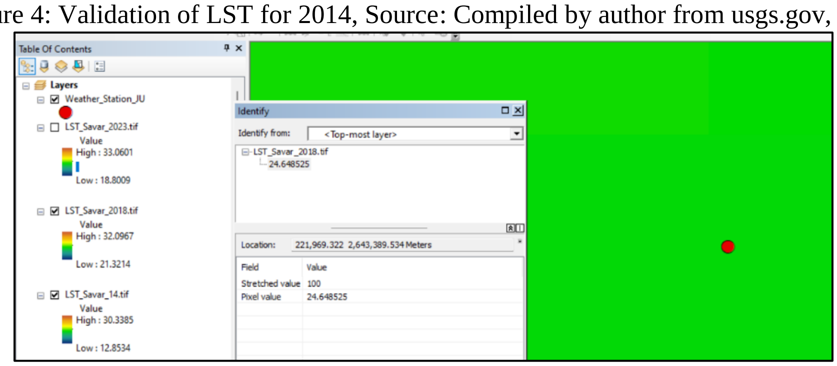

Figure 5: Validation of LST for 2018, Source: Compiled by author from usgs.gov, 2023

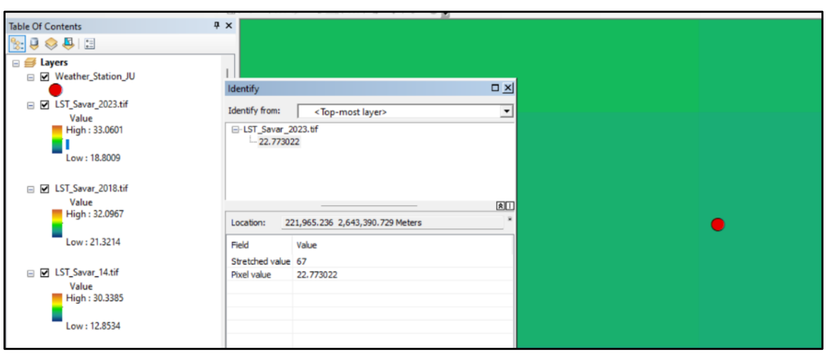

Figure 6: Validation of LST for 2023, Source: Compiled by author from usgs.gov, 2023

For better comprehension of urban heat, a link between NDVI and LST has also been depicted. The findings demonstrate that surface emissivity can be calculated using fractional vegetation cover and NDVI, and that the satellite-derived emissivity values fall within acceptable ranges. A thorough definition and proper documentation of the validation datasets applied, along with uncertainty estimates for the reference LST values (related, for instance, to the precision of the radiometric measurements, emissivity estimates, and ground-based retrieval process), should be included in the validation operations. Since geographical representativeness and directional effects are tough to correct, quantitative examination of algorithm uncertainties involves specialized, high-quality in situ LST measurements over areas that are homogeneous at the spatial scale of the satellite observation system. It is suggested that only locations that closely mirror the satellite field of view be used for validation. When coordinated in-situ and satellite-retrieved LST data sets are accessible in a common format, like that which is recommended and implemented, researchers can carry out (global) LST validation studies more methodically and efficiently. The LPV subgroup believes that as in situ survey techniques become more accessible and LST products are used more frequently in environmental research, the spatial representativeness of in situ LST data will develop.

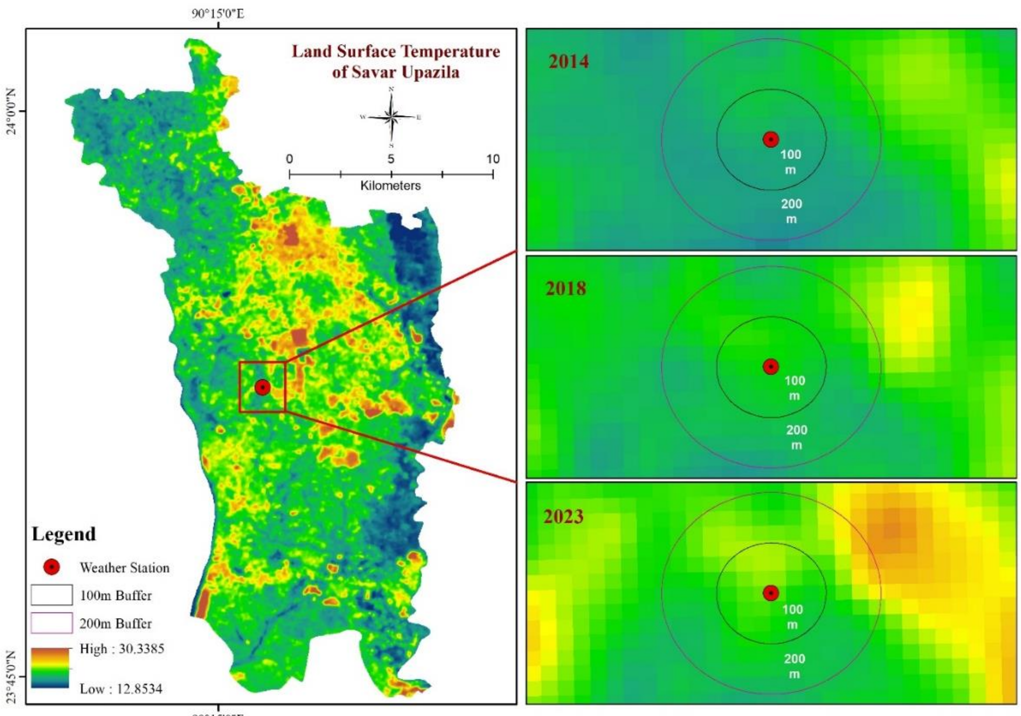

Figure 7: Created buffer zone for showing the increasing trends of LST values over the years (2014, 2018 and 2023); Source: Compiled by author from usgs.gov data, 2023

The figure 7 illustrate the buffer proximity changed over the years (2014, 2018 and 2023) and that is expressed in the different reflections in band combinations for retrieving LST, in total the temperatures changed. It helps perform spatial queries by selecting features that fall within a buffer zone around a specific point of weather observatory.

3.3 Correlation between LST and NDVI

Considering variation in the reflectance of near-infrared and visible red light, the NDVI index calculates live green vegetation in a specific area. LST is the land surface temperature as determined by remote sensing equipment. According to studies, the NDVI and LST have a negative connection, meaning that regions with more vegetation typically have lower surface temperatures. This is so that plants can offer shade and evapotranspiration, which both serve to cool the surrounding air and lessen the quantity of solar energy that is absorbed by the ground. Given that variations in vegetation cover can have a substantial impact on regional and global temperatures, the negative association between NDVI and LST has significant implications for climate change research. It can also be used to monitor and manage land use practices, such as urbanization and agriculture that can affect both NDVI and LST.

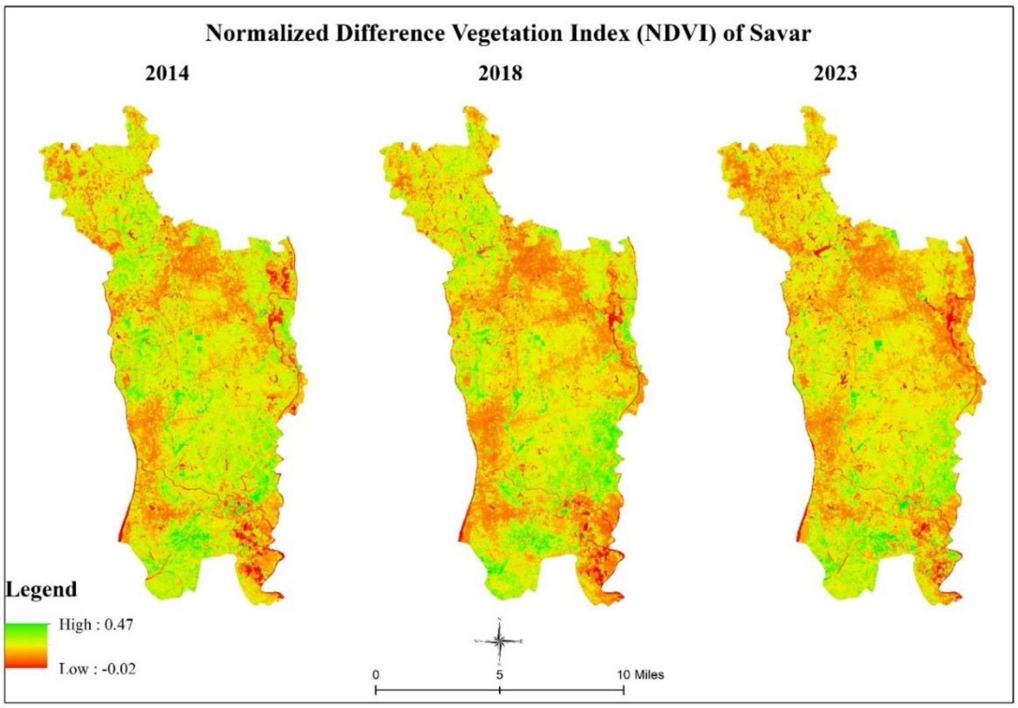

Figure 8: NDVI in Different years. Source: Compiled by author from usgs.gov, 2023

Land surface emissivity (LSE) need be calculated to estimate LST. Land surface emissivity is a measure of a surface's ability to absorb radiation in the proportional wave spectrum (Jiménez-Munoz et al., 2014). LSE is heavily influenced by the target surface top layer, such as soil type, surface roughness, and vegetation cover type (Jeevalakshmi, 2017). To calculate LSE, use the equation below. Compared to land surfaces, water bodies have a more constant emissivity. The NDVI may be applied to evaluate the emissivity of diverse land surfaces in the 10–12 m range because emissivity varies with wavelength (Mallick, Kant, and Bharath, 2008). Moreover, a link between NDVI and LST has been shown, which is particularly useful in the analysis of urban heat.

The findings demonstrate that the fractional vegetation cover and NDVI are useful in determining surface emissivity and that the satellite-derived emissivity values are within acceptable bounds.

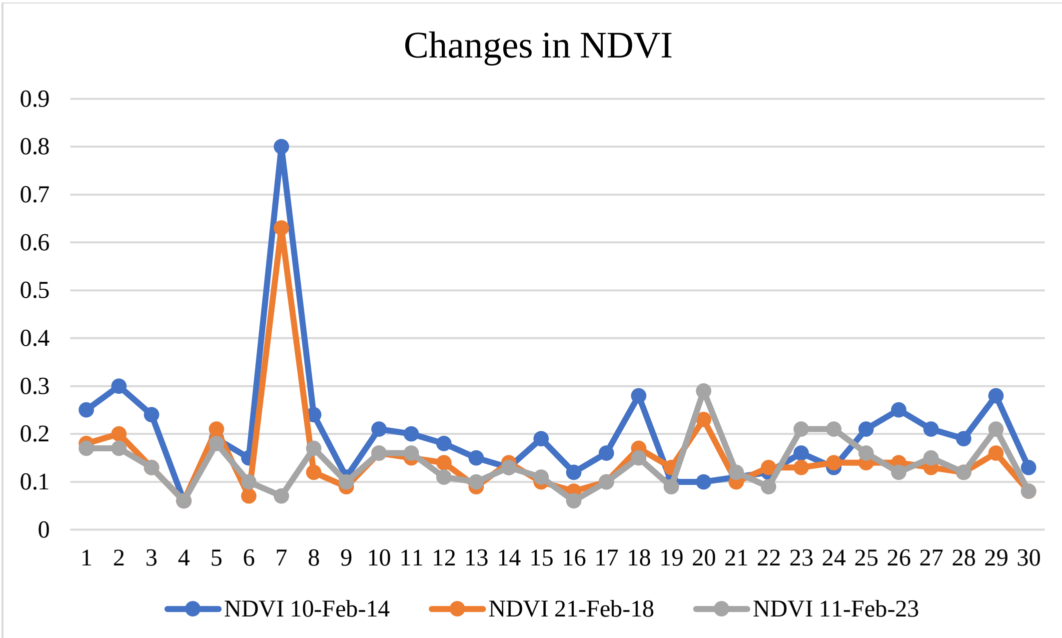

Figure 9: Trends of NDVI over the years.
Source: Compiled by author from usgs.gov data and analyzed NDVI values, 2023

Figure 9 depicts the trending pattern in NDVI which illustrates the reduction of NDVI in Savar from 2014-2023. It's quite a spectacular vision of the amount of investigation for vegetation cover or how much green reflects by the band. The quantity of green had much reduced over the 10 years, which is alarming in the sense of rapid urbanization, industrialization, and overpopulation. Population converted or changed in the livelihood pattern thus, the land acquisition and utilization had been changed. Agricultural lands had been reduced drastically and bare lands had been converted from vegetation cover. The trend sequence suspects a negative correlation with LST.

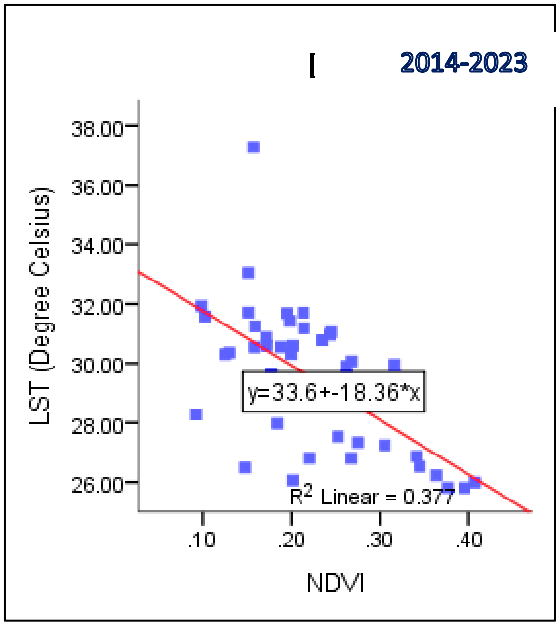

Figure 10: Scatter Plot for LST vs. NDVI,
Source: Compiled by author from usgs.gov data and analyzed NDVI values, 2023

Using statistical correlative equations, it had been observed that, NDVI had a negative link with LST observed throughout the studied period and Figure 10 showed the correlation with discard values from the temperature data.

4. Discussion

One of the major factors that characterizes surface states and processes that are significant for research on climate, hydrology, ecology, and human health is land surface temperature. This study proposed a workable technique for recovering LST from Landsat 8 TIRS data. The outcomes of the simulations represented that the suggested method can determine LST with an accuracy greater than 1.0 K. The results of a noise analysis of the measured brightness temperature, emissivity, and water vapour showed that the novel approach was effective for LST retrieval. The study illustrates how geophysical parameter distribution and intensities can be estimated using remote sensing to examine urban morphology. Understanding the broad land classes in urban regions and the challenges of the energy budget are made easier by emissivity and surface temperature. This provides causes and effects, which is a substantial improvement over the current urban environment monitoring methods. By analyzing time series data across our region of interest, future research can improve the approach for predicting LST to account for the atmospheric impact and seasonal weather variations. In addition, a relationship between NDVI and LST has been established, which is helpful in the analysis of urban heat. The results represent that the satellite-derived emissivity values are within acceptable ranges and that the fractional vegetation cover and NDVI are helpful in calculating surface emissivity. The methodology can be applied to the research of metropolitan areas because the field-measured values and the estimated surface temperature values are found to be in reasonable agreement. The LST value can specify the precise temperature value for each land cover in place of using air temperature data from meteorological stations due to the weather station's inability to completely cover a larger area and offer coverage. So, in the continuously evolving technological world, the land surface temperature is a better choice for geographers to retrieve and plan future research. For the investigation, thermal band temperatures were collected, and specific weather stations were mapped. To make the research more precise and targeted, the data is generated at a specific time. After data calculation and incorporation, the finding can be stated in degrees Celsius, and the deviation is precisely determined. Crop management, water management, interaction between the land and the atmosphere, modelling studies, changes in the composition of the land, and climate change are just a few of the uses for satellite-based Land Surface Temperature (LST) information. As a result, the temperature comparison is assessed. This finding will have extensive ramifications because temperature data can be collected and assessed from far-off, station-free locations.

5. Conclusion

Although the temperature increase is a worry, accurate figures might be obtained by using remote sensing to measure temperature. That will help researchers gather reliable data, and a comparison study has shown how much variation is noted. This study has generated accurate temperature data, developed a number of algorithms, and provided station-based information. By analysing time series data across our region of interest, future research can improve the approach for predicting LST to account for the atmospheric impact and seasonal weather variations. In addition, a relationship between NDVI and LST has been shown, which is helpful in the analysis of urban heat. As a part of the inquiry, temperatures from thermal bands were gathered and specific weather stations were mapped. To help clarify and hone the research, the data is created at a specific time. The result can be stated in degrees Celsius after computation and integration, and the difference can be precisely calculated. The temperature comparison is evaluated as a result. As temperature data from far-off and station-less sites may be recovered and studied, this conclusion has wide-ranging ramifications. Satellite-based LST observations will be useful for applications such as crop management, water management, modelling studies, land cover changes, and climatic change.

References

Ahmed, Z., Alam, R., Hussain, A. H. M. B., Ambinakudige, S., Chowdhury, T. A., Kabir, M. N., Nahin, K. T. K., & Ahmed, M. N. Q. (2022). Agricultural land conversion and land surface temperature change in four industrial areas in Bangladesh: results from remote sensing and DPSIR approach. Arabian Journal of Geosciences, 15(10). https://doi.org/10.1007/s12517-022-10049-x

Avdan, U., & Jovanovska, G. (2016). Algorithm for automated mapping of land surface temperature using LANDSAT 8 satellite data. Journal of Sensors, 2016. https://doi.org/10.1155/2016/1480307

Barzaman, S., Shamsipour, A., Lakes, T., & Faraji, A. (2022). Indicators of urban climate resilience (case study: Varamin, Iran). Natural Hazards, 112(1), 119–143. https://doi.org/10.1007/s11069-021-05174-x

Bodrud-Doza, M., Ahmed, F., Asikunnaby, Hosain, M. A., Rakib, M. A., Bhuiyan, M. A. H., & Rahman, M. S. (2016). GEO-SPATIAL ASSESSMENT OF GHGs EMISSION IN SAVAR UPAZILA, BANGLADESH. *Journal of Nature Science and Sustainable Technology*, *10*(3).

Bröde, P., Fiala, D., Błażejczyk, K., Holmér, I., Jendritzky, G., Kampmann, B., Tinz, B., & Havenith, G. (2012). Deriving the operational procedure for the Universal Thermal Climate Index (UTCI). *International Journal of Biometeorology*, *56*(3), 481–494. https://doi.org/10.1007/s00484-011-0454-1

Caselles, V., Artigao, M. M., Hurtado, E., Coll, C., & Brasa, A. (1998). Mapping actual evapotranspiration by combining Landsat TM and NOAA-AVHRR images: Application to the barrax area, Albacete, Spain. *Remote Sensing of Environment*, *63*(1), 1–10. https://doi.org/10.1016/S0034-4257(97)00108-9

Chen, X. L., Zhao, H. M., Li, P. X., & Yin, Z. Y. (2006). Remote sensing image-based analysis of the relationship between urban heat island and land use/cover changes. *Remote Sensing of Environment*, *104*(2), 133–146. https://doi.org/10.1016/j.rse.2005.11.016

Chowdhury, M. A., Zzaman, R. U., Tarin, N. J., & Hossain, M. J. (2022). Spatial variability of climatic hazards in Bangladesh. *Natural Hazards*, *110*(3), 2329–2351. https://doi.org/10.1007/s11069-021-05039-3

Dash, P., Göttsche, F. M., Olesen, F. S., & Fischer, H. (2002). Land surface temperature and emissivity estimation from passive sensor data: Theory and practice-current trends. *International Journal of Remote Sensing*, *23*(13), 2563–2594. https://doi.org/10.1080/01431160110115041

Hashim, B. M., Al Maliki, A., Sultan, M. A., Shahid, S., & Yaseen, Z. M. (2022). Effect of land use land cover changes on land surface temperature during 1984–2020: a case study of Baghdad city using landsat image. *Natural Hazards*, *112*(2), 1223–1246. https://doi.org/10.1007/s11069-022-05224-y

Hottel, H. C., & Broughton, F. P. (1932). Determination of True Temperature and Total Radiation from Luminous Gas Flames: Use of Special Two-Color Optical Pyrometer. *Industrial and Engineering Chemistry - Analytical Edition*, *4*(2), 166–175. https://doi.org/10.1021/ac50078a004

Igun, E., & Williams, M. (2018). Impact of urban land cover change on land surface temperature. Global Journal of Environmental Science and Management, 4(1), 47-58.

Imran, H. M., Hossain, A., Islam, A. K. M. S., Rahman, A., Bhuiyan, M. A. E., Paul, S., & Alam, A. (2021). Impact of Land Cover Changes on Land Surface Temperature and Human Thermal Comfort in Dhaka City of Bangladesh. *Earth Systems and Environment*, *5*(3), 667–693. https://doi.org/10.1007/s41748-021-00243-4

Imran, H. M., Hossain, A., Shammas, M. I., Das, M. K., Islam, M. R., Rahman, K., & Almazroui, M. (2022). Land surface temperature and human thermal comfort responses to land use dynamics in Chittagong city of Bangladesh. *Geomatics, Natural Hazards and Risk*, *13*(1), 2283–2312. https://doi.org/10.1080/19475705.2022.2114384

Kakon, A. N., Mishima, N., & Kojima, S. (2009, December). Simulation of the urban thermal comfort in a high density tropical city: Analysis of the proposed urban construction rules for Dhaka, Bangladesh. In Building Simulation (Vol. 2, pp. 291-305). Springer Berlin Heidelberg.

Kamran, K. V., Pirnazar, M., Bansouleh, V. F., & Azarbayjan, E. (2015). *Land Surface Temperature retrieval from Landsat 8 TIRS- comparison between Split Window algorithm and SEBAL method*. *9535*, 1–12. https://doi.org/10.1117/12.2192491

Lagouarde, J.-P., Kerr, Y. H., & Brunet, Y. (1995). An experimental study of angular effects on surface temperature for various plant canopies and bare soil. *Agricultural and Forest Meteorology*, *77*(3–4), 167–190.

Lo, C. P. (1997). Application of LandSat TM data for quality of life assessment in an urban environment. *Computers, Environment and Urban Systems*, *21*(3–4), 259–276. https://doi.org/10.1016/S0198-9715(97)01002-8

Mansor, S. B., Cracknell, A. P., Shilin, B. V., & Gornyi, V. I. (1994). Monitoring of underground coal fires using thermal infrared data. *International Journal of Remote Sensing*, *15*(8), 1675–1685. https://doi.org/10.1080/01431169408954199

Marajh, L., & He, Y. (2022). Temperature Variation and Climate Resilience Action within a Changing Landscape. *Remote Sensing*, *14*(3). https://doi.org/10.3390/rs14030701

Module 1 : Global Policy Context for Climate Change. (n.d.).

Monserud, R. A., & Leemans, R. (1992). Comparing global vegetation maps with the Kappa statistic. Ecological modelling, 62(4), 275-293.

Ogunjobi, K. O., Adamu, Y., Akinsanola, A. A., & Orimoloye, I. R. (2018). Spatio-temporal analysis of land use dynamics and its potential indications on land surface temperature in Sokoto Metropolis, Nigeria. Royal Society open science, 5(12), 180661.

Oppenheimer, C. (1997). Remote sensing of the colour and temperature of volcanic lakes. *International Journal of Remote Sensing*, *18*(1), 5–37. https://doi.org/10.1080/014311697219259

Qin, Z., Karnieli, A., & Berliner, P. (2001). A mono-window algorithm for retrieving land surface temperature from Landsat TM data and its application to the Israel-Egypt border region. *International Journal of Remote Sensing*, *22*(18), 3719–3746. https://doi.org/10.1080/01431160010006971

Qin, Zhihao, & Karnieli, A. (1999). Progress in the remote sensing of land surface temperature and ground emissivity using NOAA-AVHRR data. *International Journal of Remote Sensing*, *20*(12), 2367–2393. https://doi.org/10.1080/014311699212074

Rehman, A., Qin, J., Pervez, A., Khan, M. S., Ullah, S., Ahmad, K., & Rehman, N. U. (2022). Land-Use/Land Cover Changes Contribute to Land Surface Temperature: A Case Study of the Upper Indus Basin of Pakistan. *Sustainability (Switzerland)*, *14*(2). https://doi.org/10.3390/su14020934

Ritchie, J. C., Cooper, C. M., & Schiebe, F. R. (1990). The relationship of MSS and TM digital data with suspended sediments, chlorophyll, and temperature in Moon Lake, Mississippi. *Remote Sensing of Environment*, *33*(2), 137–148. https://doi.org/10.1016/0034-4257(90)90039-O

Rozario, S. R., Rezaie, A. M., & Khan, M. R. (2021). Insights on land use, agriculture and food security in Bangladesh: way forward with climate change and development. *Agriculture for Development*, *44*(6).

Rozenstein, O., Qin, Z., Derimian, Y., & Karnieli, A. (2014). *Derivation of Land Surface Temperature for Landsat-8 TIRS Using a Split Window Algorithm*. 5768–5780. https://doi.org/10.3390/s140405768

Saraf, A. K., Prakash, A., Sengupta, S., & Gupta, R. P. (1995). Landsat-tm data for estimating ground temperature and depth of subsurface coal fire in the jharia coalfield, india. *International Journal of Remote Sensing*, *16*(12), 2111–2124. https://doi.org/10.1080/01431169508954545

Schmugge, T., French, A., Ritchie, J. C., Rango, A., & Pelgrum, H. (2002). Temperature and emissivity separation from multispectral thermal infrared observations. *Remote Sensing of Environment*, *79*(2–3), 189–198. https://doi.org/10.1016/S0034-4257(01)00272-3

Shi, T., Huang, Y., Wang, H., Shi, C. E., & Yang, Y. J. (2015). Influence of urbanization on the thermal environment of meteorological station: Satellite-observed evidence. *Advances in Climate Change Research*, *6*(1), 7–15. https://doi.org/10.1016/j.accre.2015.07.001

Sobrino, J. A., Caselles, V., & Becker, F. (1990). Significance of the remotely sensed thermal infrared measurements obtained over a citrus orchard. *ISPRS Journal of Photogrammetry and Remote Sensing*, *44*(6), 343–354. https://doi.org/10.1016/0924-2716(90)90077-O

Sobrino, J A, & Mattar, C. (n.d.). *Calibration and Validation of land surface temperature for Landsat8- TIRS sensor TIRS LANDSAT-8 CHARACTERISTICS*.

Sobrino, José A., Jiménez-Muñoz, J. C., & Paolini, L. (2004). Land surface temperature retrieval from LANDSAT TM 5. *Remote Sensing of Environment*, *90*(4), 434–440. https://doi.org/10.1016/j.rse.2004.02.003

Study Area Savar View of Industrial Development and Climate Change_ A Case Study of Bangladesh.pdf. (n.d.).

Taylor, P., Kaneko, D., & Hino, M. (n.d.). *International Journal of Remote Sensing Proposal and investigation of a method for estimating surface energy balance in regional forests using TM derived vegetation index and observatory routine data*. *December 2014*, 37–41. https://doi.org/10.1080/01431169608949074

Taylor, P., Sobrino, J. A., Li, Z., Stoll, M. P., & Becker, F. (n.d.). *International Journal of Remote Sensing Multi-channel and multi-angle algorithms for estimating sea and land surface temperature with ATSR data*. *September 2012*, 37–41.

Tomlinson, C. J., Chapman, L., Thornes, J. E., & Baker, C. (2011). Remote sensing land surface temperature for meteorology and climatology: A review. *Meteorological Applications*, *18*(3), 296–306. https://doi.org/10.1002/met.287

Unknown_Unknown_Journal of Applied Meteorology 1992 Barton.pdf.pdf. (n.d.).

V.A.R.Barao, R.C.Coata, J.A.Shibli, M.Bertolini, & J.G.S.Souza. (2022).

Weng, Q., Liu, H., & Lu, D. (2007). Assessing the effects of land use and land cover patterns on thermal conditions using landscape metrics in city of Indianapolis, United States. *Urban Ecosystems*, *10*(2), 203–219. https://doi.org/10.1007/s11252-007-0020-0

Weng, Q., Lu, D., & Schubring, J. (2004). Estimation of land surface temperature-vegetation abundance relationship for urban heat island studies. *Remote Sensing of Environment*, *89*(4), 467–483. https://doi.org/10.1016/j.rse.2003.11.005

Zhang, T., Zhou, Y., Zhu, Z., Li, X., & Asrar, G. R. (2022). A global seamless 1km resolution daily land surface temperature dataset (2003-2020). *Earth System Science Data*, *14*(2), 651–664. https://doi.org/10.5194/essd-14-651-2022

Zhang, X., Van Genderen, J. L., & Kroonenberg, S. B. (1997). A method to evaluate the capability of Landsat-5 TM band 6 data for sub-pixel coal fire detection. *International Journal of Remote Sensing*, *18*(15), 3279–3288. https://doi.org/10.1080/014311697217080